Cross-Polarization Magic-Angle Spinning ^{13}C Nuclear Magnetic Resonance Study of the Homogeneity of Some Photopolymerized Acrylic Networks

A. Lungu and D. C. Neckers*

Center for Photochemical Sciences,[1] Bowling Green State University, Bowling Green, Ohio 43403

Received June 9, 1995; Revised Manuscript Received September 14, 1995[⊗]

ABSTRACT: A theoretical analysis of relaxation processes has been used in the qualitative interpretation of carbon-resolved, proton $T_{1\rho}$ data obtained at 100.56 MHz for three solid polyacrylate networks made by photopolymerization of the polyol acrylate monomers poly(ethylene glycol) diacrylate (PEGA), trimethylolpropane triacrylate (TMPTA), and dipentaerythritol pentaacrylate (DPHPA). This analysis permits an estimate of the spin diffusion rates between different chemical species. Such rates are strongly dependent on spatial proximity and hence are applicable to the determination of the homogeneity of the networks. Proton $T_{1\rho}$'s in networks are not quite averaged to a single value by spin diffusion like in polymer blends, indicating there is extensive intermixing of TMPTA and DPHPA in forming the network. Proton $T_{1\rho}$ experiments are sufficiently sensitive to distinguish between a TMPTA/DPHPA network and PEGA homopolymer. When glass fibers are present in the network, they act like a spin diffusion medium, producing an increase in the rates of relaxation for all three components of the network.

Introduction

The introduction of polyacrylates for the rapid formation of clear polymers when exposed to UV light in the presence of certain small molecular photoinitiators traces to Plambeck who developed their use in preparing relief images for printing plates. According to the original patent one of the most widely used photoengraving processes at the time (1956) was to expose metals coated with very thin layers of gelatins photosensitive to light through an image-bearing transparency, thus forming the reverse image in the photosensitive layers.[2] Plambeck's contribution was to recognize that multifunctionality in an acrylate ester would force cross-linking, and thus produce a more rapid photoresponse. In a British patent,[3] relief forms for printing were produced from methyl methacrylate, the primary monomer of Plexiglas, in an image-forming manner, followed by a thermal step.

As critical as polyol acrylates such as TMPTA, DPHPA, and pentaerythritol tetraacrylate (PETA) are in commerce,[4] little is known about the actual structures of polymers formed from them. Photopolyol acrylates are commercial, and they work for the purposes for which they were intended. Further, unraveling the structures of complex network polymers is a difficult task. This is in direct contrast to the first negative photoresists, the poly(vinyl cinnamates) developed by Minsk,[5] van Deusen, and Robertson at Eastman Kodak[6] the photoproducts from which have been characterized completely by Reiser in a series of now classical works in photopolymer science.[7]

For several years we have been concerned with understanding the relationship between the photochemistry and photophysics of the photoinitiators and the coinitiators used to form photopolymers with visible light and the physical properties of the polymers they form. The impetus for this is the use of photopolymerization processes in the formation of shapes by stereolithography. The mechanical properties of the formed photopolymers have direct implications for the use to which the objects formed by stereolithography can be put.

Among the structural characteristics of poly(polyol acrylates) of interest is how the cross-linking density relates to the diffusion rate of solvent or monomer through formed polymers, to their hardness, and to other physical properties. We also anticipate that by determining the relative reactivity of individual monomers, and the individual carbons in those monomers, we can understand the features of molecular architecture which determine physical properties.

Cross-polarization magic-angle spinning (CPMAS) ^{13}C NMR provides information about both the structure and the dynamics of atomic motion of a variety of solid polymers.[8–13] Resolved isotropic chemical shifts identify chemical environments, and these may be unique to the solid state. Relaxation experiments exploit this high resolution so that ^{13}C T_1's and $T_{1\rho}$'s can be used to characterize individual main- and side-chain motions in the megahertz- and kilohertz-frequency ranges, respectively.[14,15]

The high-resolution magic-angle techniques used to obtain ^{13}C NMR spectra in solids can also be employed to measure individual $T_{1\rho}$'s for protons attached to various carbon atoms in the polymer. This is possible because the final evolution of the carbon signal in a cross-polarization experiment tracks the $T_{1\rho}$ decay of the protons.[10] Neither the cross-relaxation between carbons and protons nor the strong homonuclear coupling between protons (12–20 kHz) is affected by mechanical spinning (5 kHz).[8] Through spin diffusion, proton $T_{1\rho}$'s of a multicomponent system are strongly dependent on the short range (1–2 nm) spatial proximity, or mixing, of the various components. Measuring a proton $T_{1\rho}$ by monitoring a resolved carbon resonance is therefore well suited to structural analysis in the complicated class of polymeric solids known as networks.

In solid polymers proton relaxation is often perturbed by spin diffusion.[16] Because of this process, which tends to average different relaxations, all protons often share the same relaxation time and the individual relaxation characteristics are lost. In heterogeneous systems,

[⊗] Abstract published in *Advance ACS Abstracts,* November 1, 1995.

0024-9297/95/2228-8147$09.00/0

however, the influence of spin diffusion on proton relaxation times can be very useful. For example, in a polymer network formed from two or more different components, all the protons may or may not average to a common relaxation time if the rate of spin diffusion (determined by the domain size and the spin diffusion constant[17]) is large compared with the difference between the component polymers. If instead the rate of spin diffusion is small compared to the difference in relaxation rates (large domains/small diffusion constant), the components of the network retain their relaxation behavior.

In this paper we report the results of high-resolution ^{13}C NMR experiments on three different formulations of acrylate networks. These experiments lead to new qualitative conclusions regarding both the intimacy and homogeneity of mixing of the individual polyacrylate monomers in these materials.

Experiments

General Information. The polymers used in this study were formed by the photopolymerization of three different formulations of acrylate monomers. The monomers used in these formulations were poly(ethylene glycol)-400, diacrylated (from Monomer-Polymer Laboratories, Inc.) with $M_w = 400$; trimethylolpropane triacrylate (Sartomer 357, from Sartomer Co.); and dipentaerythritol pentaacrylate (Sartomer 399, from Sartomer Co.). Monomer stabilizers were not removed because doing so generates an instability in the reaction mixture, and the polymerization commences before it is intended. Each monomer was used without further purification. It was confirmed by ^{13}C NMR spectra that the purities of the monomers are 97.5% (PEGA), 96.8% (TMPTA), and 92.7% (DPHPA).

Irradiation was carried out with an Ar^+ laser (Omnichrome 543−200 MGS). The photoinitiator was 2,4-diiodo-6-butoxy-3-fluorone hereafter DIBF[15] used at concentrations which varied from 5×10^{-4} to 1×10^{-3} M. *N,N*-Dimethyl-2,6-diisopropylaniline, [DIDMA] (from Carbolabs, Inc.), was used as the electron donor at concentrations varying from 3×10^{-3} to 0.1 M.

We assigned the carbon peaks by comparing the liquid NMR spectra with those obtained from solid-state NMR. Therefore the assignments are CH_3 carbon from TMPTA (7.2 ppm), CH_2−O carbons from DPHPA (64.1 ppm), and CH_2−O carbons from PEGA (72.2 ppm).

Sample Preparation. The formulations had the following compositions: formulation 1, called "TD" contains 50% TMPTA and 50% DPHPA; formulation 2, called "STDR" contains 40% TMPTA, 40% DPHPA, and 20% PEGA; formulation 3, called "filled" had the same composition as "STDR", but also contained 10% glass fiber ($^1/_{32}$ in. milled fibers from Fiber Glast). The glass fiber was milled and passed through a filtermesh with 50 nm holes. All the percentages are by weight.

Reactive mixtures were poured into dogbone-shaped Teflon molds, and the laser beam was directed toward the sample by mirrors positioned above the molds. The mirrors were controlled by $x-y$ scanners (DX-series servo controller, from General Scanning, Inc.) driven by digitized computer data from a special file which traced over a bit more than a 200.0 × 200.0 mm square region. This region is large enough to cover the entire dogbone-shaped mold. Laser power was varied from 40 to 150 mW, and the scan speed was 8.0 mm/s. After the irradiation was complete, the photopolymerized dogbones were frozen in liquid nitrogen and crushed.

CPMAS NMR. Solid-state ^{13}C CPMAS NMR spectra were recorded at 100.56 MHz using a Varian UnityPlus 400 spectrometer equipped with a high-power amplifier and a Varian CPMAS probe. Samples were packed as powders in silicon nitride rotors with Kel-f endcaps and spun at the magic angle with a spinning rate of 6.0 kHz at 290 K. Cross-polarization was performed at 33 kHz (7.5 μs 90° pulses for both ^{13}C and ^1H), the proton-decoupling strength was approximately 63 kHz, and the delay between successive acquisitions was 5 s. The cross-polarization contact time was varied between 0.3 and 25 ms. All spectra were collected at room temperature (20 °C) since our instrument does not have a variable temperature probe. Therefore all the spectra were recorded below the T_g for all the polymers.

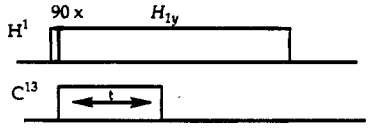

Figure 1. Cross-polarization pulse sequence used in the experiments.

Results

The cross-polarization pulse sequence used in the experiments is shown in Figure 1. Proton $T_{1\rho}$ relaxation can be characterized by means of matched spin-locked, cross-polarization experiments.[8] After initial, rapid buildup of carbon polarization, the carbon signal tracks the polarization in the proton reservoir and thus follows its decrease via the $T_{1\rho}(H)$ process. Under high-resolution conditions, the individual carbon resonances follow the protons to which they are most closely coupled and thus are capable of resolving $T_{1\rho}(H)$ differences between protons which might be difficult to detect if the $T_{1\rho}$ process were obtained directly from the composite proton signal.[10] The CPMAS spectra of the three formulations are shown in Figure 2a−c.

In the case of the "TD" type network, a decrease in the rotating-frame spin−lattice relaxation time constant was observed for all the protonated carbons from a plot of the variation of the $T_{1\rho}(H)$ with the laser power used for photopolymerization, Figure 3a. The error bars for the $T_{1\rho}(H)$ values are ±0.12−0.16 ms. In Figure 3b we present the percentages of the double bond conversion, as a function of laser power, for TMPTA and DPHPA, as determined previously by IR.[18] These data suggest the spin diffusion between the two components, TMPTA and DPHPA, increases with an increase in the laser power. As was pointed out previously, the cross-linking density is directly related to the laser power.[18] Therefore, the network has a higher degree of cross-linking at the high laser power, and the chains are less mobile. Since the network with a higher degree of cross-linking has a number of "holes" in its structure, and less mobility of its chains, spin diffusion is more efficient at high laser power. In the case of the "STDR" polymer, an increase in the $T_{1\rho}(H)$ values with the laser power was observed for all the protonated carbons when PEGA was added to the initial mixture of TMPTA and DPHPA. In each case, an increase in the proton $T_{1\rho}$ with an increase of laser power from 40 mW to approximately 80 mW was observed, while a decrease was observed at higher laser powers. This suggests that the presence of PEGA decreases the rate of spin diffusion between all three components of the mixture.

PEGA, which contains only two acrylic groups, has a lower rate of polymerization than does either TMPTA or DPHPA with three and five acrylic groups, respectively. Since PEGA is large in comparison with either TMPTA or DPHPA, in diffusion-controlled cross-linking reactions, the reactivity of PEGA becomes diffusion limited first and its reactivity drops more quickly than does that of TMPTA or DPHPA. At relatively low laser powers (40−80 mW), PEGA gives a degree of double bond conversion close to 20%, as measured by the disappearance of the 810 cm^{-1} stretching frequency in

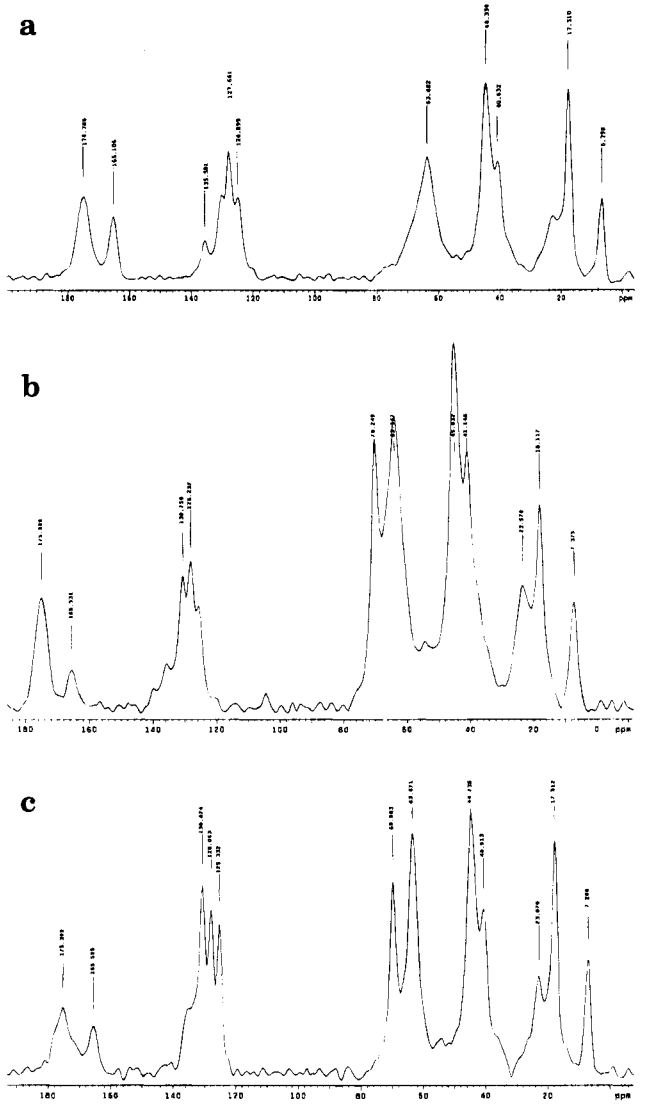

Figure 2. (a) CPMAS ^{13}C spectrum of the "TD" type formulation. (b) CPMAS ^{13}C spectrum of the "STDR" type formulation. (c) CPMAS ^{13}C spectrum of the "filled" type formulation.

the infrared spectrum.[18] Since this indicates the samples to be not well polymerized, individual PEGA units have significant mobility and can be separated from the network. This inhibits the spin diffusion process and produces an enhancement in the rotating-frame spin–lattice relaxation time constants, Figure 4a. The error bars for the $T_{1\rho}$(H) values are ±0.08–0.22 ms. Double bond conversions for all the monomers present in the "STDR" mixtures are given in Figure 4b.[19]

These oligomeric units of PEGA act like a plasticizer when added to the "TD" mixture. At low laser powers (60–80 mW) the PEGA is not polymerized, and its chains are close to the network formed by TMPTA and DPHPA. This improves the spin diffusion process; therefore the proton $T_{1\rho}$ values increase for all three monomers. When the laser power reaches a threshold value, the PEGA begins to participate in the network, and the mobility of its carbons decreases. Consequently, a decrease in the rotating-frame spin–lattice relaxation time constant is observed at higher laser powers.

Similar results are observed when the mechanical properties of the "STDR" polymer are studied.[19] Introduction of PEGA, with only two possible branching groups and separated by relatively long distances (much greater than the distance between the acrylic groups

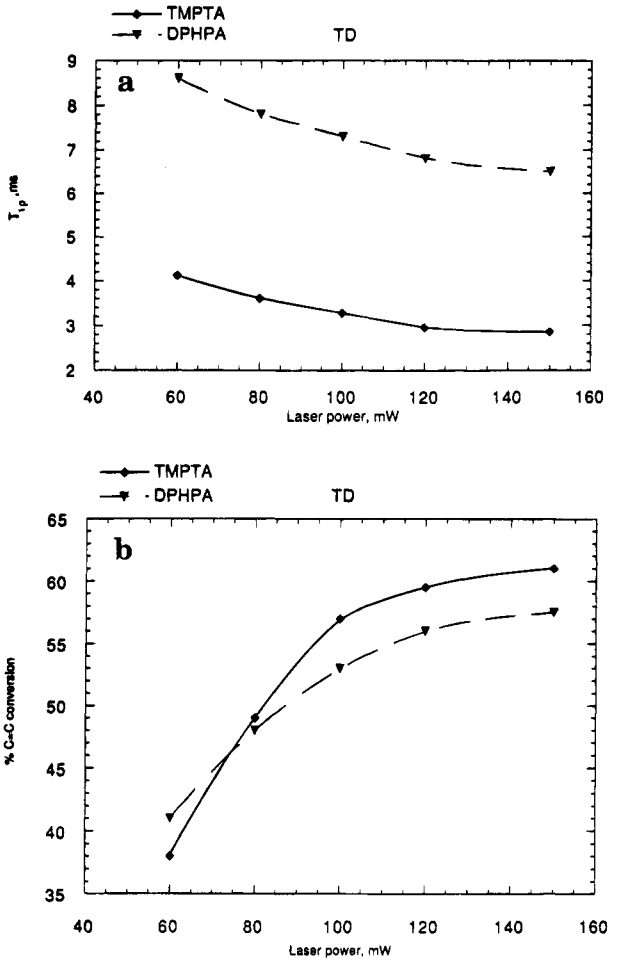

Figure 3. (a) TMPTA and DPHPA proton $T_{1\rho}$ variation with the laser power in the "TD" type of network. (b) TMPTA and DPHPA double bond conversions in the "TD" type of network.

in TMPTA and DPHPA), is expected to decrease the cross-link density, which is one of the major factors in determining the mechanical strength of networked polymeric materials.[20] Therefore, by decreasing the cross-link density, both the stress-at-break (σ) and Young's modulus also decrease.[19]

The fluctuations in $T_{1\rho}$ indicate that there are two types of polymer motion which induce relaxation. Both become increasingly restricted as the cross-link density increases. As the frequency of one motion approaches the spin-lock field strength, it becomes efficient at inducing relaxation. With increased cross-linking both types of motion have mismatched frequencies relative to the spin-lock field; one motion is too slow, and the second is too fast. Further cross-linking at the highest laser powers finally slows the second type of motion to the frequency which matches the spin-lock field, where it becomes efficient at inducing relaxation and results in reduction of proton $T_{1\rho}$.

In the case of the "filled" system in which the monomers are those of the "STDR" system to which 10% glass fibers have been added, a smaller increase in the $T_{1\rho}$(H) values with laser power is observed for all the protonated carbons as compared to "STDR", Figure 5a. The error bars in this case are ±0.1–0.14. Double bond conversions for the monomers present in the "filled" system are presented in Figure 5b.[19] The proton $T_{1\rho}$ values increase until the laser power reaches the value of 60–80 mW, and after that a continuous decrease is observed in all cases. In this system, the mobility of

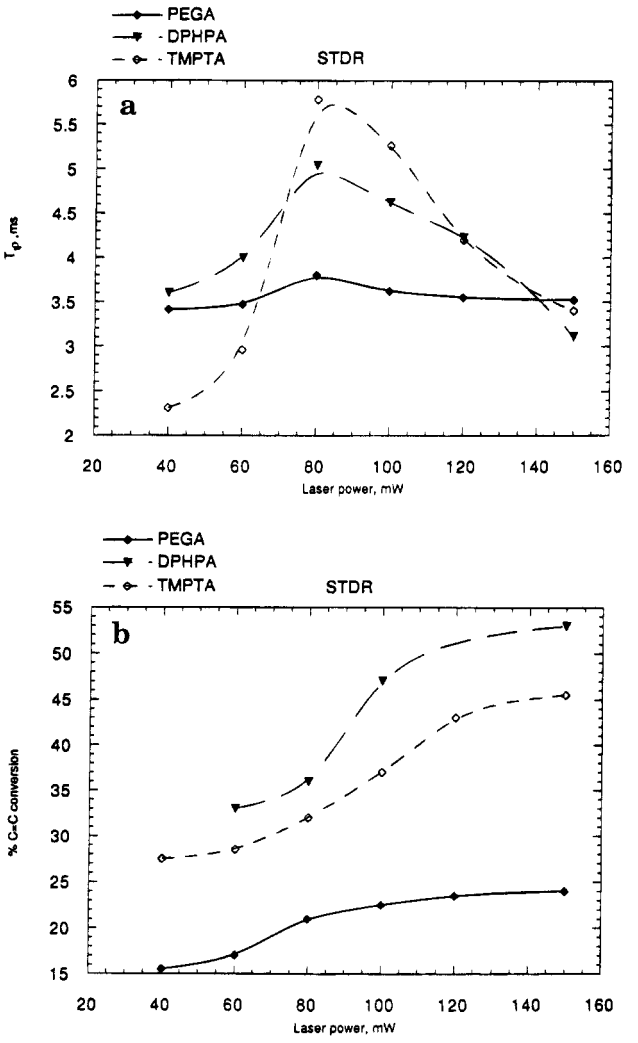

Figure 4. (a) PEGA, TMPTA, and DPHPA proton $T_{1\rho}$ variation with the laser power in the "STDR" type of network. (b) PEGA, TMPTA, and DPHPA double bond conversions in the "STDR" type of network.

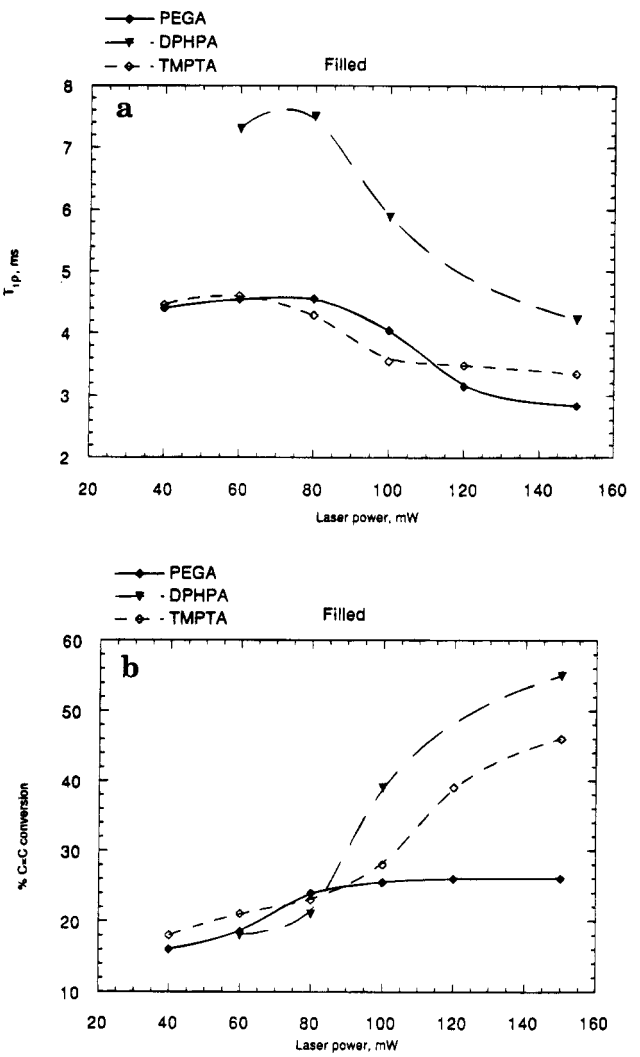

Figure 5. (a) PEGA, TMPTA, and DPHPA proton $T_{1\rho}$ variation with the laser power in the "filled" type of network. (b) PEGA, TMPTA, and DPHPA double bond conversions in the "filled" type network.

the nonpolymerized units of PEGA is reduced due to the presence of the glass fibers. Since the network with the reinforced material, the "filled" system, has less mobility than the "STDR", the increase in the $T_{1\rho}$(H) values with the laser power is smaller in the former than in the latter case. Also, as in the case of the "STDR" formulation, after a certain value of the laser power, where the PEGA begins to polymerize, the proton $T_{1\rho}$ values decreased with an increase in the irradiation intensity, due to the fact that the rate of spin diffusion is smaller in this case.

With the pulse sequence of Figure 1, the carbon magnetization, M, is given by[10]

$$dM/dt = \{[M_0 e^{-t/T_{1\rho}(H)} - M]/T_{IS} - M/T'_{\rho L}\} \quad (1)$$

where M_0 is the maximum carbon polarization available in a matched spin-lock experiment with no dissipative processes, $T_{1\rho}$(H) is the rotating-frame spin−lattice relaxation time constant, T_{IS} is the proton−carbon matched spin-lock cross-polarization time constant, and $T'_{\rho L}$ is the carbon rotating-frame spin−lattice relaxation time constant in the presence of dipolar decoupling of the protons. Thus

$$M = (M_0/T_{IS})[e^{-t/T_{1\rho}(H)} - e^{-t(1/T_{IS}+1/T_{\rho L})}]/[1/T_{IS} + 1/T'_{\rho L} - 1/T_{1\rho}(H)] \quad (2)$$

and since $T'_{\rho L} \gg T_{IS}$ the following approximation can be made

$$M \approx (M_0/T_{IS})[e^{-t/T_{1\rho}(H)} - e^{-t/T_{IS}}]/[1/T_{IS} - 1/T_{1\rho}(H)] \quad (3)$$

Moreover, since $T_{1\rho}(H) > T_{IS}$ when $t \gg T_{IS}$

$$M \sim M_0 e^{-t/T_{1\rho}(H)}/[1 - T_{IS}/T_{1\rho}(H)] \quad (4)$$

Therefore, from a semilog plot of magnetization (M) vs contact time (t), we obtain $T_{1\rho}$(H).

It is also the case that $T_{1\rho}$(H) measurements can describe the homogeneity of intimate acrylic networks. Modeling such relaxation behavior can be done by considering that the protons may be divided into two species (in the case of "TD" formulation) or three species (in the case of "STDR" and "filled" formulations), depending on which polymer they are part of (PEGA, TMPTA, or DPHPA).

In the "TD" case, if we use "T" for TMPTA protons and "D" for DPHPA protons, the equations describing $T_{1\rho}$(H) relaxation are

$$-dT/dt = (K_T + f_D k_c)T - f_T k_c D$$

$$-dD/dt = (K_D + f_T k_c)D - f_D k_c T \quad (5)$$

where, if n_T and n_D represent the numbers of T and D spins, respectively, $f_T = n_T/(n_T + n_D)$ and $f_D = n_D/(n_T + n_D)$ represent the fractions of T and D spins.[21] The three rate constants K_T (the initial decay rate of TMPTA protons before cross-relaxation), K_D (the initial decay rate of DPHPA protons), and k_c (the cross-relaxation rate) are defined by

$$K_T = 2n_T\langle W_2\rangle_{TT} + 2n_D\langle W_2\rangle_{TD}$$

$$K_D = 2n_D\langle W_2\rangle_{DD} + 2n_T\langle W_2\rangle_{TD}$$

$$k_c = (n_T + n_D)(\langle W_0\rangle_{TD} - \langle W_2\rangle_{TD}) \quad (6)$$

In these equations, W_2 represents the probability that a pair of interacting protons will each flip so as to make $\Delta m = \pm 1$ and W_0 represents the probability of a pair of flips resulting in $\Delta m = 0$. The averages are pairwise between spins of the species indicated by the subscripts. There are no terms involving W_1 since $\Delta m = \pm 1/2$ flips are not important.[22] The probabilities $\langle W_0\rangle_{TT}$ and $\langle W_0\rangle_{DD}$ are not very small but contribute to neither net relaxation nor cross-relaxation and thus drop out. These probabilities do describe the spin diffusion within species T and D, which makes it possible to regard each species as homogeneous.[23] These equations are an extension of the treatment of relaxation due to Solomon.[24]

If initially at $t = 0$, $T = T_0$, $D = D_0$, and $T_0/D_0 = n_T/n_D$, the solution of the coupled relaxation equations has the following form

$$T = t_+ e^{r_+ t} + t_- e^{r_- t}$$

$$D = d^+ e^{r_+ t} + d_- e^{r_- t} \quad (7)$$

where

$$r_\pm = {}^1/_2[-(K_T + K_D + k_c) \pm R]$$

$$t_\pm = {}^1/_2 T_0[1 + R^{-1}(K_D + k_c - K_T)]$$

$$d_\pm {}^1/_2 D_0[1 \pm R^{-1}(K_T + k_c - K_D)]$$

$$R = +\{[(K_T - K_D) + (f_D - f_T)k_c]^2 + 4f_T f_D k_c^2\}^{1/2} \quad (8)$$

As was noted earlier, K_T and K_D represent the initial rates of relaxation. However, as time passes, cross-relaxation pulls the relaxation rates together until both T and D relax at the same intermediate rate.[10]

The same approach was applied in the case of "STDR" and "filled" formulations, where K_P is the initial rate of relaxation for PEGA protons.

Fitting data magnetization vs contact time is just a matter of determining the initial slopes for each species and then adjusting k_c until the remainder of the decay curves are fitted satisfactorily.

$T_{1\rho}$(H) in the "TD" Type Network. The relaxation rates for PEGA homopolymer, TMPTA homopolymer, and DPHPA homopolymer, at different laser powers, are almost constant: $K_P = 12\ s^{-1}$, $K_T = 42\ s^{-1}$, and $K_D = 72\ s^{-1}$, Table 1.

Table 1. Relaxation Rates for PEGA Homopolymer (K_P), TMPTA Homopolymer (K_T), and DPHPA Homopolymer (K_D), at Different Laser Powers

laser power, mW	K_P, s^{-1}	K_T, s^{-1}	K_D, s^{-1}
40	12.02 ± 0.8	41.24 ± 1.6	71.65 ± 2.2
60	11.86 ± 0.6	42.33 ± 1.8	71.71 ± 2.8
80	11.92 ± 0.7	42.18 ± 2.0	72.44 ± 2.3
100	12.31 ± 0.7	42.36 ± 1.9	72.18 ± 2.5
120	12.50 ± 0.6	41.87 ± 2.0	71.04 ± 2.3
150	11.81 ± 0.7	42.06 ± 1.8	72.31 ± 2.4

Table 2. Relaxation Rates for TMPTA (K_T) and DPHPA (K_D) in the 'TD' Type of Formulation, at Different Laser Powers

laser power, mW	K_T, s^{-1}	K_D, s^{-1}	k_c, s^{-1}
60	46 ± 1.7	68.6 ± 2.9	102
80	48.2 ± 1.8	55.1 ± 2.4	100
120	45.1 ± 1.3	53.2 ± 2.2	98
150	47.3 ± 1.6	49.4 ± 2.4	85

Table 3. Relaxation Rates for PEGA (K_P), TMPTA (K_T), and DPHPA (K_D) in the "STDR" Type of Formulation, at Different Laser Powers

laser power, mW	K_P, s^{-1}	K_T, s^{-1}	K_D, s^{-1}	k_c, s^{-1}
40	10 ± 0.3	43 ± 1.7	49 ± 1.9	184
60	7 ± 0.1	34 + 1.6	43 + 1.1	186
100	7 ± 0.5	40 ± 1.4	45 ± 1.2	190
120	8 ± 0.6	41 ± 1.4	53 ± 1.3	185
150	10 ± 0.2	47 ± 1.6	55 ± 1.7	188

Since there are two types of polymer motion which induce relaxation, one fast and one slow, we report the relaxation rates only for the slow type. For the faster type, $T_{1\rho}$ decreases at very short times and so the initial slopes for each species cannot be determined by this method.

Table 2 shows the results of fitting the data for "TD" for four different laser powers. The values of K_T and K_D required to fit the "TD" data are clearly intermediate between the homopolymer rates. This suggests that $\langle W_2\rangle_{TD}$ makes a significant contribution to the initial relaxation rates.[10] That is, mixing is intimate enough that TMPTA relaxation is aided by interaction with nearby, efficiently relaxing DPHPA, and DPHPA relaxation is reduced by its dispersal in TMPTA.

This explanation is more plausible than one that says that dispersal is not complete but molecular motions are altered by blending. An explanation based on changes in motion would require that TMPTA speed up and DPHPA slow down even though they were not intimately mixed. While, in an intimate mixture, it is possible that some coming together of rates of motion may occur, it is more likely that proton density differences between TMPTA and DPHPA give rise to the shifts in K_T and K_D on blending. The size of k_c also suggests an intimate mixing of the two species of protons. Also, by increasing the laser power (more than 120 mW), the values of the two rates of relaxation are coming closer.

This suggests that the two monomers are forming a network which is becoming more and more homogeneous at larger laser powers.

$T_{1\rho}$(H) in the "STDR" Type Network. The semilog plot data of the magnetization vs contact time is presented for this type of network at different laser powers in Table 3. Although the fit was as good as with the "TD" data, the fitting parameters do not seem reasonable when compared to the "TD" parameters. In

Table 4. Relaxation Rates for PEGA (K_P), TMPTA (K_T), and DPHPA (K_D) in the "Filled" Type of Formulation, at Different Laser Powers

laser power, mW	K_P, s^{-1}	K_T, s^{-1}	K_D, s^{-1}	k_c, s^{-1}
60	10.6 ± 0.4	74.6 ± 2.5	180 ± 5.3	173
100	12.3 ± 0.3	72.3 ± 2.9	176.8 ± 6.1	179
120	15.4 ± 0.7	72.6 ± 2.1	153 ± 6.0	191
150	15.2 ± 0.6	90.7 ± 3.8	110.0 ± 4.4	182

"STDR" we have a mixture in which K_P and K_T resemble more closely the homopolymer values, while k_c indicates greater cross-relaxation. Around 60 mW the initial decay rate for TMPTA protons starts to slow down. This is due to a decrease in the mobility of the monomeric units; subsequently, the TMPTA units are bonding to the DPHPA units forming the network. Since K_P has a smaller value thatn K_T and K_D, PEGA must be in relatively poor contact with the TMPTA/DPHPA network.

The increase in k_c cannot be caused by a proton density change since the "TD" mixture is denser than "STDR". We solve this discrepancy by attributing part of the initial decay of the PEGA protons to small regions where the PEGA is not fully dispersed, and hence these protons relax more like those of the PEGA homopolymer. The net result is a phase separation between the solid network and the PEGA homopolymeric gel. By increasing the laser power, the DPHPA and TMPTA start to speed up due to their intimate contact with the mobile long chains of PEGA. K_P is still low because of the dispersal of PEGA chains in the network's cages. These regions of poorly dispersed PEGA need not be more than places where awkwardly kinked long chains of PEGA homopolymer tend to fold back on themselves.[10] The resulting regions are in less contact with the nearby network so that an effective phase separation can occur. At higher laser power, the PEGA starts to bond inside the cages, and the spin diffusion is more effective now (K_P is increasing).

$T_{1\rho}$(H) in the "Filled" Type Network. The variations of the rates of relaxation for PEGA protons, TMPTA protons, and DPHPA protons with the laser power in the system in which we added glass fibers in the "STDR" type network are presented in Table 4. In this case all the rates have larger values than in the case of "STDR", but the same phase separation is observed between the PEGA homopolymer and TMPTA/DPHPA network, since k_c has pretty high values.

The bigger values and the fact that the PEGA is speeding up as the laser power is increased are caused by the presence of the glass fibers which can act like a "catalyst" for the spin diffusion process. These glass fibers keep the interactions between the monomers during the polymerization process "constant". The same increase in the homogeneity of the network with laser power was observed (K_P and K_D values are coming closer).

Perhaps the presence of the glass fibers induces some chemical modifications in the "filled" system, since the effect of the fibers should be rather small at the spatial scales probed by NMR relaxation times, although the size of the fibers is around 50 nm.

Acknowledgment. This work has been supported by the National Science Foundation (DMR-9013109) and the Office of Naval Research (N00014-93-1-0772). The NMR spectrometer used in these experiments was purchased with funds from grants from the NSF (CHE9302619), the Ohio Board of Regents, and Bowling Green State University. We are most grateful for the support of these agencies. Conversations with Afranio Torres-Filho are gratefully acknowledged.

References and Notes

(1) Contribution No. 237 from the Center for Photochemical Sciences.
(2) Plambeck, L. F., Jr. U.S. Patent 2,760,863, August 28, 1956, et seq. to E. I. DuPont de Nemours and Co., Wilmington, DE. See: Neckers, D. C. *Historical Readings in Photochemistry*; SPIE Press: Bellingham, WA, 1993.
(3) Gates, British Patent, 566,795, January 15, 1945.
(4) Current estimates indicate markets for all photopolymerization technologies worldwide to exceed $1,000,000,000/year.
(5) Minsk, L. M. U.S. Patent 2,725,377, 1955.
(6) Minsk, L. M.; van Deusen, W. P.; Robertson, E. M. U.S. Patent 2,610,120, September 1952.
(7) Reiser, A.; Egerton, P. L. *Macromolecules* **1979**, *12*, 670. Egerton, P. L.; Reiser, A.; Pitts, E. *Macromolecules* **1981**, *14*, 95. Egerton, P. L.; Trigg, J.; Hyde, E. M.; Reiser, A. *Macromolecules* **1984**, *14*, 100.
(8) Schaefer, J.; Stejskal, E. O.; Buchdahl, R. *Macromolecules* **1977**, *10*, 384.
(9) Dejean de la Batie, R.; Laupretre, F.; Monnerie, L. *Macromolecules* **1988**, *21*, 2045.
(10) Stejskal, E. O.; Schaefer, J.; Sefcik, M. D.; McKay, R. A. *Macromolecules* **1981**, *14*, 275.
(11) Dong, L.; Hill, D. J. T.; Whittaker, A. K.; Ghiggino, K. P. *Macromolecules* **1994**, *27*, 5912.
(12) Bahani, M.; Laupretre, F.; Monnerie, L. *J. Polym. Sci. Polym. Phys. Ed.* **1995**, *33*, 167.
(13) O'Donnell, J. H.; Whittaker, A. K. *J. Polym. Sci., Polym. Chem. Ed.* **1992**, *30*, 185.
(14) Gerard, A.; Laupretre, F.; Monnerie, L. *Polymer* **1994**, *35*, 3402.
(15) Axelson, D. E.; Mandelkern, L.; Levy, G. C. *Macromolecules* **1977**, *10*, 557.
(16) McBierty, V. J.; Douglas, D. C. *J. Polym. Sci., Macromol. Rev.* **1981**, *16*, 295.
(17) Schantz, S.; Ljunqvist, N. *Macromolecules* **1993**, *26*, 6517.
(18) Torres-Filho, A.; Neckers, D. C. *J. Appl. Polym. Sci.* **1994**, *51*, 931.
(19) Torres-Filho, A.; Neckers, D. C. *Chem. Mater.* **1995**, *7*, 744.
(20) Berlin, A. A.; Matvejava, N. G. *J. Polym. Sci., Macromol. Rev.* **1980**, *15*, 107.
(21) Stejskal, E. O.; Schaefer, J.; Steger, T. R. *Symp. Faraday Soc.* **1979**, *13*, 56.
(22) Jones, G. P. *Phys. Rev.* **1966**, *148*, 332.
(23) Brooks, A. A.; Cutnell, J. D.; Stejskal, E. O.; Weiss, V. W. *J. Chem. Phys.* **1968**, *49*, 1571.
(24) Solomon, I. *Phys. Rev.* **1955**, *99*, 559.

MA950820+